The Meteorological Society of Japan

Scientific Online Letters on the Atmosphere (*SOLA*)

EARLY ONLINE RELEASE

This is a PDF of a manuscript that has been peer-reviewed and accepted for publication. As the article has not yet been formatted, copy edited or proofread, the final published version may be different from the early online release.

The DOI for this manuscript is

DOI: 10.2151/sola.2022-040.

J-STAGE Advance published date: November 11, 2022

The final manuscript after publication will replace the preliminary version at the above DOI once it is available

SOLA, 2022, Vol.18, 235-238, doi: 10.2151/sola.2022-040

Global warming effect and adaptation for a flooding event at Motsukisamu River in Sapporo

Yuka Kanamori[1], Masaru Inatsu[2], Ryoichi Tsurumaki[3], Naoki Matsuoka[3], Tsuyoshi Hoshino[4] and Tomohito J. Yamada[5]

[1]*Sapporo Regional Headquarters, Japan Meteorological Agency, Sapporo, Japan*

[2]*Faculty of Science and Center for Natural Hazards Research, Hokkaido University, Sapporo, Japan*

[3]*Hokkaido Weather Technology Center Co. Ltd., Sapporo, Japan*

[4]*Civil Engineering Research Institute for Cold Region, Sapporo, Japan*

[5]*Faculty of Engineering and Center for Natural Hazards Research, Hokkaido University, Sapporo, Japan*

(Submitted to *Scientific Online Letters on the Atmosphere* on 10 September 2022 and in a revised form on 13 October 2022)

Corresponding author: Masaru Inatsu, Hokkaido University, N10W8, Kita-ku, Sapporo, Hokkaido, Japan, 060-0810. E-mail: inaz@sci.hokudai.ac.jp

Abstract

A set of hydrological experiments for a flooding event on September 11, 2014 at Motsukisamu River in Sapporo were performed. Dynamical downscaling to 5-km resolution of a large-ensemble global simulation allowed us to estimate that a 99%-tile hourly precipitation in Sapporo would increase by 70% in a future climate, when the global-mean temperature increases by 4 K compared with the present climate. After developing a three-tank model of which parameters were optimized on the basis of the in-situ observation at the Motsukisamu River during the event period, the model was forced by hypothetical hyetographs of the event that would occur under the future climate. The results of this experiment suggested that the peak flow rate would increase by 75%. However, it was also revealed that an upstream aqueduct tunnel, just completed in autumn 2021, would effectively reduce the peak flow rate and mitigate the flooding risk even in extreme precipitation under the future climate.

1. Introduction

Many reported that extreme precipitation was intensified with the recent temperature increase (Peterson et al. 2008; Westra et al. 2013; Fujibe 2013). The global climate model simulation projected the increase in extreme precipitation over most of the mid-latitude land-masses in a warmer climate (IPCC AR5 WG1). Global flood projections showed flood hazards increasing over East-to-South Asia, in spite of great variability at the catchment scale (Dankers et al. 2014; Hirabayashi et al. 2013). On the other hand, flood risk of local river basins to climate changes has been recently assessed by a river model tuned individually and then forced by many possible hyetographs provided by a large ensemble climate-model simulation (Hoshino and Yamada, 2018;

Tachikawa et al. 2017). Hoshino et al. (2020) evaluated the characteristics of tropical cyclones that induced heavy rainfall over the Tokachi River basins in Hokkaido, Japan. This technique can be applied to relatively smaller river basins in Hokkaido (Nguyen et al. 2021).

As introduced above, the assessment of flooding risk to climate change was established for rivers with their catchment area larger than 100,000 km^2 by global models (Hirabayashi et al. 2021) and even for river basins > 1,000 km^2 with dynamical downscaling. However, it remains challenging to assess smaller river basins like urban rivers. A hindrance is attributed to difficulty to accurately simulate meso-scale convective systems that bring torrential rainfall such as squall lines and rainbands by atmospheric models even with 1-km resolution. Although the extreme precipitation is reproduced statistically with a 5-km resolution model (Sasaki et al. 2011), the model is hardly to reproduce the occurrence probability and short-time variability of these phenomena and let alone its change in a warmer climate. Another difficulty in the assessment of small-scale river basins is to find feasible modeling approaches amid the lack of rainfall and discharge observations (Grimaldi et al. 2021); Despite no assurance on its simplification, the tank model was widely used for its convenience to be easily fit with an event in an arbitrary river. Recently, Yoshioka et al. (2020) attempted to evaluate the flood risk of an urban river in Tokyo, by utilizing a large-ensemble dynamically-downscaled data.

The purpose of this study is to evaluate the impact of climate change to a small urban river. In order to mitigate the former difficulty, we proposed an idea combining gauged precipitation and a change ratio from model simulations focusing a particular torrential rainfall event. We here assumed that, if the same event occurred under the global warming environment, the rainfall intensity would only depend on the content of water vapor in the atmosphere. Although regional climate models cannot accurately reproduce all the events, we estimated the change ratio as the difference of extreme precipitation intensity between present and future climate simulations. In order to tackle the latter difficulty, we targeted the Motsukisamu River, running through residential areas of Sapporo, Hokkaido, Japan (Figs. 1a,b). We focus on the event of the river flooding on September 11, 2014, due to torrential rainfall associated with a line-shaped rainband (Kato 2020), elongated along the direction from southwest to northeast over central Hokkaido. The rainfall amount at this event strongly depended on the location of the rainband, so that we also used other hyetographs observed near the site under the assumption that the rainband were horizontally shifted. Furthermore, this study evaluates the effect of an aqueduct tunnel in the upstream of the Motsukisamu river (Fig. 1c).

2. Data and Methods

2.1 In-Situ Observation

We used the in-situ observation data of the water level and rainfall at a downstream point of the Motsukisamu River (43.0317°N, 141.3861°E; Fig. 1c) by Hokkaido Weather Technology Center. Rainfall has been observed with a tipping bucket rain gauge with 0.5 mm error, and the water level has been observed with hydraulic crystal water gauge with 0.1%FS error. The data were a 10-minute interval.

We also used the rainfall data with a 10-minute interval of Automated Meteorological Data Acquisition System (AMeDAS) observation sites by the Japan Meteorological Agency. The nearest site is Sapporo (43.06°N, 141.33°E), but we used other 11 sites in Ishikari subprefecture of Shinshinotsu (43.22°N, 141.65°E), Yamaguchi (43.15°N, 141.22°E), Teineyama (43.08°N, 141.20°E), Koganeyu (42.96°N, 141.22°E), Eniwa-Shimamatsu (42.93°N, 141.57°E), Shikotsukohan (42.77°N, 141.41°E), Ishikari (43.19°N, 141.37°E), Hamamasu (43.58°N, 141.39°E), Atsuta (43.40°N, 141.44°E), Chitose (42.78°N, 141.69°E), and Ebetsu (43.11°N, 141.60°E; Fig. 1b).

2.2 Downscaling Data

The database for Policy Decision-Making for Future Climate Change (d4PDF) dataset contained a large ensemble simulation by the Meteorological Research Institute Atmospheric General Circulation Model, version 3.2 (Mizuta et al. 2012) with a horizontal resolution of 60 km and the dynamical downscaling by Non-Hydrostatic Regional Climate Model (Sasaki et al. 2011; Murata et al. 2013) covering the Japanese territory with a horizontal resolution of 20 km. The number of ensembles is 100 for the historical 1950-2010 simulation and 90 for the future climate simulation, where the global-mean surface temperature increases by 4 K relative to the preindustrial period.

In this study, we used the further dynamical downscaling results to a horizontal resolution of 5 km covering Hokkaido Island (Hoshino and Yamada, 2018). This was conducted for selected years in the d4PDF ensembles with the heaviest 72-hour precipitation totals in the Tokachi River basin between 1 June and 1 December. Because the probability density of hourly precipitation in the 20-km d4PDF data at Sapporo was independent of the selection of years related to precipitation over the Tokachi River basin (Fig. 2a), we regarded this selection as random sampling. In total, 769 years from 3000 years of the historical simulation and 735 years from 5400 years of the future simulation were downscaled from 20-km resolution d4PDF dataset. Among them, we statistically analyzed hourly precipitation data at the nearest grid-point to the observation site at the Motsukisamu River (the southwest blue point in Fig. 1c).

2.3 River Model

We developed a three-tank model for the domain (6.61 km^2), upstream to the monitoring site (green point in Fig. 1c), which predicted runoff and ground water flow rates (Sugawara 1972, 1995). The parameters of runoff coefficients, penetration coefficients, and heights of tank holes (Appendix A) were optimized with differential evolution (Storn and Price 1997), based on precipitation and water level observed at the Motsukisamu River site on September 11, 2014. The flow rate Q (m^3 s^{-1}) was converted into water level H (m) by the following formula based on observation:

$$Q = \begin{cases} 12.50\,(H - 34.80)^2 & (34.80 \leqq H \leqq 34.90) \\ 24.91\,(H - 34.83)^2 & (34.90 < H \leqq 35.06) \\ 12.94\,(H - 34.74)^2 & (35.06 < H) \end{cases} \quad (1)$$

We included the effect of the aqueduct tunnel in this three-tank model. Considering the capability and location of the tunnel, we divided the rainfall forcing into the upstream basin (S_1 = 4.78×10^6 m^2) from the tunnel entrance (72% of the total catchment area) and the downstream (28%): $R_{\mathrm{in}} = 0.72\,R_{\mathrm{rm}} + 0.28\,R_{\mathrm{ob}}$, where R_{ob} [mm (10 min)$^{-1}$] is observed precipitation, and R_{rm} [mm (10 min)$^{-1}$] is the upstream-oriented precipitation after drainage. The upstream water flowed out following an overflow formula that had been obtained by the statistical fitting based on measurement of flow and water level in hydraulic model experiments for the design of aqueduct tunnel entrance:

$$\begin{cases} Q_1 = -3.0650 \times 10^{-4} Q_0^2 + 0.94947 Q_0 - 1.7005 \\ \qquad\qquad\qquad\qquad (Q_0 \leq 50) \\ Q_1 = -1.1381 \times 10^{-2} \min(Q_0, Q_a)^2 + 1.8566 \min(Q_0, Q_a) - 19.303 \\ \qquad\qquad\qquad\qquad (Q_0 > 50) \end{cases} \quad (2)$$

where Q_0 and Q_1 are the inflow just before the tunnel and the outflow to the tunnel and

Q_a is 58.5 m^3 s^{-1}.

2.4 Experiments

We performed the historical and future experiments with the three-tank model forced by precipitation in the flooding event on September 11, 2014, or its processed one. The reference historical experiment was a hindcast experiment with on-site rainfall itself (Section 2.1). In addition, we performed "ensemble" historical experiments with possible hyetographs hypothesized that the line-shaped rainband were horizontally shifted. This was done by the same three-tank model but forced by AMeDAS rainfall data at 12 different sites.

The future experiments were also performed with possible hyetographs hypothesized that the flooding event occurred in future environment. The hyetograph was simply created by the procedure that the rainfall amount in all the timeframes was multiplied by 1.70. This rate was computed by the ratio of a 99%-tile value of hourly precipitation exceeding 0.1 mm threshold in June-July-August-September months at the nearest grid-point to the Motsukisamu observation site from 735-year future simulation with 5-km resolution to that from 769-year historical simulation. We used this value as the multiplying factor, because the historical simulation almost reproduced the extreme statistics of hourly precipitation and the ratio was comparable for higher precipitation intensity like the target event with a 99.95%-tile value at the peak (Fig. 2b). The "ensemble" future experiments were also done with 12 AMeDAS rainfall data multiplied by 1.70.

3. Results

First, we validated the three-tank model specially tuned to the flooding event by the differential evolution method with the learning data of water levels estimated by the H-Q relation [Eq. (1)] from 00:00 10 September to 24:00 11 September. The reference historical experiment with the input precipitation observed at the Motsukisamu River site on the date showed a reasonable variation of hydrograph, compared with the observed at the same site (Fig. 3a). There were two peaks in hyetograph exceeded 8 mm $(10\ \text{min})^{-1}$ at 2:00-2:20 and 3:30-4:20 on this date (Hereafter time is in Japanese Standard time). The observed and simulated hydrographs showed that the peaks were emerged almost at the same timing but with a 10-minute delay to the precipitation peak surpassed 36.30 m, the flood stage level 4. The torrential rainfall ceased at 8:00 there. The simulated water level dropped to the baseline soon[1], while the observed one was gradually declined.

Figure 3b displays the hyeto-hydrograph of the "ensemble" historical experiments with hypothesized precipitation at 12 different AMeDAS sites in Ishikari area that would occur at the Motsukisamu river basin. We here paid attention to two sites at Shikotsukohan and Chitose, quite close to the line-shaped rainband. At Shikotsukohan the rainfall exceeded 15 mm $(10\ \text{min})^{-1}$ in two periods, the first around 5:30 and the second around 18:45. In the hypothesized experiment with this rainfall data given to the

---

[1] The flow rather than water level tended to show a peaky graph (not shown), so that the fitting likely took a stronger influence from the larger flow around the peak. Hence, we made light of an error around the weak flow, or water levels near baseline. We guess that other possible reasons are the heavier rainfall in the upstream that we did not cope with and some leakage in the river that was not well reproduced in this simple tank model.

Motsukisamu River model, the water level attained local maxima in the peak rainfall period there. The first peak was 37.3 m and the second peak exceeded 37.5 m. A similar hyetograph was found in Chitose, with a secondary rainfall peak in 23:00. In the hypothesized experiment, secondary flooding would have happened at the Motsukisamu River in this second rainfall peak. Because rainfall data in other sites have a similar variation but with an unclear peak, the result of ensemble simulation showed the water level would increase in the period during 2:00-6:00 but would not likely attain the flooding level.

The result of the future reference simulation is shown in Fig. 4a. Accompanied with the heavier rainfall, the simulation showed spiky peaks of runoff almost at the same timing as the rainfall peaks. The peak flow rate was 1.75 times higher. Similarly, the "ensemble" simulation showed more spiky peaks of runoff and the water level would approach to the flood stage level 4 if some AMeDAS points were replaced with (Fig. 4b).

Finally, we assessed the effect of the aqueduct tunnel effect to the water level at the Motsukisamu River. The reference historical experiment with the tunnel effect revealed that the peak water level would be much lower than the flood stage level 4 (Fig. 5a). Even in the reference experiment, the tunnel effect would significantly reduce the peak water level (Fig. 5b). Hence it can be indicated that the aqueduct tunnel is a treatment of flood risk in the present climate as well as an adaptation of the future climate.

4. Discussion

The assessment of climate change effect to a small urban river has been challenging, but the technique proposed here is so simple that it could be highly versatile for the urban rivers where the hyeto-hydro graph was available with enough a shorter sampling interval compared to the rainfall-runoff timescale. We targeted a specific flood event and used a lumped model to avoid hydrological uncertainty in the urban-river modeling. If one attempted to make a more accurate and more universal river model to use any flooding events with a sophisticated manner like distributed models, a stumbling block would be the necessity of densely distributed verification data. Moreover, an accurate urban-river modeling needed complete inflow/outflow information of a city drainage network. Because it seemed virtually impossible to resolve these problems in the present engineering level, this study is considered to be the best-effort approach to the flood-risk assessment of small urban rivers.

A caveat of our method is a rough estimate of hyetograph for the target event that would occur in the global warming environment. Even if a meteorological phenomenon that brought extreme rainfall occurred under a warmer climate, a simple multiplication of rainfall amount without any other changes in the hyetograph would not be warrant. To relieve this problem, one possible way is to use pseudo global warming (PGW) dynamical downscaling (Sato et al. 2007), in which the boundary conditions are obtained by adding the future-to-present difference estimated by GCM into observed data. However, even state-of-the-art atmospheric models cannot always well reproduce the meso-scale convection system. Even though the model were capable to reproduce the system, its possible few-kilometer shift would be critical for the estimate of urban river input. These are reasons why we avoided a PGW method in this paper.

5. Conclusions

We adopted an idea of simple multiplication of precipitation amount in a heavy rainfall event and assessed the flooding risk at the Motsukisamu River in Sapporo under a warmer climate. First, we checked that extreme precipitation at Sapporo increased by 70% in future climate where the global-mean temperature increases by 4 K, based on dynamical downscaling to 5-km resolution of a large-ensemble global simulation called d4PDF. Next, we validated that a three-tank model driving the observed precipitation during the target period of a flood event at the Motsukisamu River. The river model forced by hypothetical hyetographs of the event that would occur under the future climate as a manner of PGW experiment suggested that the peak flow rate would increase by 75%. It was also revealed that the upstream aqueduct tunnel would effectively reduce the peak flow rate and mitigate the flooding risk even in extreme precipitation under the future climate.

Acknowledgement

MI and TJY are supported by JSPS KAKENHI grant 19H00963, by JPMXD0717935457 and JPMXD0722680734 of Ministry of Education, Sports, Culture, Science and Technology (MEXT), and by Research Field of Hokkaido Weather Forecast and Technology Development (endowed by Hokkaido Weather Technology Center Co. Ltd.). MI was also funded by the Environment Research and Technology Development Fund JPMEERF20192005 of the Environmental Restoration and Conservation Agency of Japan. We used d4PDF produced with the Earth Simulator of the Japan Agency for Marine-Earth Science and Technology jointly by the MEXT science programs SOUSEI, TOUGOU, and SI-CAT. We expressed our gratitude Mr. Yoshimichi Tachikawa and Mr. Hidenori Yamahira to provide us the detailed hydrological information on the aqueduct tunnel and Dr. Yousuke Sato to give a technical assistance for handling meteorological data. Figure 1c was based on Map of Geospatial Information Authority of Japan with

some modifications.

Appendix A. Tank model and the parameters

We implemented the standard three-tank model that consists of a set of prognostic equation of storage of first, second and third tanks, S_1, S_2, and S_3, forced by rainfall R as

$$\begin{aligned} \frac{dS_1}{dt} &= -\beta_1 S_1 - q_1(t) + R, \\ \frac{dS_2}{dt} &= -\beta_2 S_2 - q_2(t) + \beta_1, \\ \frac{dS_3}{dt} &= -\beta_3 S_3 - q_3(t) + \beta_2, \end{aligned} \tag{A1}$$

and

$$\begin{aligned} q_1(t) &= \alpha_1(S_1(t) - L_1) + \alpha_2(S_1(t) - L_2), \\ q_2(t) &= \alpha_3(S_3(t) - L_3), \\ q_3(t) &= \alpha_4(S_4(t) - L_4). \end{aligned} \tag{A2}$$

The coefficients of outflow from the lower side hole in the first tank are $\alpha_1 = 1.79476$ hr^{-1} and $\alpha_2 = 0.21718$ hr^{-1}, respectively; Those from the side hole in the second and third tanks are $\alpha_3 = 1.27943$ hr^{-1} and $\alpha_4 = 1.13114$ hr^{-1}, respectively. The coefficients of leakage from the bottom hole in the first, second and third tanks are $\beta_1 = 3.32828$ hr^{-1}, $\beta_2 = 4.10502$ hr^{-1} and $\beta_3 = 4.67506$ hr^{-1}, respectively. The heights of the lower and upper side hole in the first tank are L_1 =0.77872 mm and L_2 =9.40112 mm, respectively; Those of the side hole in the second and third tanks are L_3 =0.01223 mm and L_4 =10.39208 mm, respectively.

References

Dankers, R., N. W. Arnell, D. B. Clark, P. Falloon, B. M. Fekete, S. N. Gosling, J. Heinke , H. Kim, Y. Masaki, Y. Satoh, and T. Stacke, 2014: First look at changes in flood hazard in the Inter-Sectoral Impact Model Intercomparison Project ensemble. *Proceedings of the National Academy of Sciences*, **111**, 3257−3261.

Fujibe, F., 2013: Clausius-Clapeyron-like relationship in multidecadal changes of extreme short-term precipitation and temperature in Japan. *Atmospheric Science Letters*, **14**, 127−132.

Grimaldi, S., F. Nardi, R. Piscopia, A. Petroselli, and C. Apollonio, 2021: Continuous hydrologic modelling for design simulation in small and ungauged basins: A step forward and some tests for its practical use. *Journal of Hydrology*, 595, 125664.

Hirabayashi, Y., R. Mahendran, S. Koirala, L. Konoshima, D. Yamazaki, S. Watanabe, and S. Kanae, 2013: Global flood risk under climate change. *Nature Climate Change*, **3**, 816–821.

Hirabayashi, Y., M. Tanoue, O. Sasaki, X. D. Zhou, and D. Yamazaki, 2021: Global exposure to flooding from the new CMIP6 climate model projections. *Scientific Report*, **11**, 3740.

Hoshino, T., T. J. Yamada, 2018: Analysis of annual maximum precipitation over first-class river domains in Japan using a large-ensemble dataset (d4PDF). *Journal of Japan society of civil engineers Series B1*, **74**, 187−192 (in Japanese).

Hoshino, T., T. J. Yamada, and H. Kawase, 2020: Evaluation for characteristics of tropical cyclone induced heavy rainfall over the sub-basins in the Central Hokkaido, Northern Japan by 5-km large ensemble experiments. *Atmosphere*, **11**, 435.

Intergovernmental Panel on Climate Change (IPCC), 2013: Climate Change 2013: The Physical Science Basis. Contribution of Working Group I to the fifth assessment report of the Intergovernmental Panel on Climate Change. *Cambridge University Press*, Cambridge, United Kingdom and New York, NY, USA, 1535 pp.

Jinnouchi, Y., Y. Mogamiya, H. Kenmotu, and M. Hayashi, 2008: Experiment to fix the design of save diversion facilities in extreme flood at super-critical flow river. *Advances in river engineering*, published by Japan Society of Civil Engineers, **14**, 283−288 (in Japanese).

Kato, T., 2020: Quasi-stationary band-shaped precipitation systems, named “senjo-kousuitai”, causing localized heavy rainfall in Japan. *Journal of the Meteorological Society of Japan*, **98**, 485−509.

Mizuta, R., H. Yoshimura, H. Murakami, M. Matsueda, H. Endo, T. Ose, K. Kamiguchi, M. Hosaka, M. Sugi, S. Yukimoto, S. Kusunoki, and A. Kitoh, 2012: Climate simulations using MRI-AGCM3.2 with 20-km grid. *Journal of the Meteorological Society of Japan*, **90A**, 233−258.

Mizuta, R., A. Murata, M. Ishii, H. Shiogama, K. Hibino, N. Mori, O. Arakawa, Y. Imada, K. Yoshida, T. Aoyagi, H. Kawase, M. Mori, Y. Okada, T. Shimura, T. Nagatomo, M. Ikeda, H. Endo, N. Nosaka, M. Arai, C. Takahashi, K. Tanaka, T. Takemi, Y. Tachikawa, K. Temur, Y. Kamae, M. Watanabe, H. Sasaki, A. Kitoh, I. Takayabu, E. Nakakita, and M. Kimoto, 2017: Over 5,000 years of ensemble future climate simulations by 60-km global and 20-km regional atmospheric models. *Bulletin of the American Meteorological Society*, **98**, 1383−1398.

Murata, A., H. Sasaki, M. Hanafusa, and K. Kurihara, 2013: Estimation of urban heat island intensity using biases in surface air temperature simulated by a nonhydrostatic regional climate model. *Theoretical and Applied Climatology*, **112**, 351–361.

Nguyen, T. T., M. Nakatsugawa, T. J. Yamada, and T. Hoshino, 2021: Flood inundation assessment in the low-lying river basin considering extreme rainfall impacts and topographic vulnerability. *Water*, **13**, 896.

Peterson, T. C., X. B. Zhang, M. Brunet-India, and J. L. Vazquez-Aguirre, 2008: Changes in North American extremes derived from daily weather data. *Journal of Geophysical Research*, **113**, D07113. DOI:10.1029/2007JD009453

Sasaki, H., A. Murata, M. Hanafusa, M. Oh'izumi, and K. Kurihara, 2011: Reproducibility of present climate in a non-hydrostatic regional climate model nested within an atmosphere general circulation model. *Scientific Online Letters on the Atmosphere*, **7**, 173–176.

Sato, T., F. Kimura, and A. Kitoh, 2007: Projection of global warming onto regional precipitation over Mongolia using a regional climate model. *Journal of Hydrology*, **33**, 144–154.

Sugawara, M., 1972: A Method for Runoff Analysis. *Kyoritsu Shuppan Press* (in Japanese).

Sugawara, M., 1995: Tank model. Computer models of watershed hydrology, *VP Singh, ed*, *Water Resources Publications*, Chapter 6.

Tachikawa, Y., K. Miyawaki, T. Tanaka, K. Yorozu, M. Kato, Y. Ichikawa, and S. Kim, 2017: Future change analysis of extreme floods using large ensemble climate simulation data. *Journal of Japan society of civil engineers Series B1*, **73**, 77–90 (in Japanese).

Taylor, K.E., R. J. Stouffer, and G. A. Meehl, 2012: An overview of CMIP5 and the experiment design. *Bulletin of American Meteorological Society*, 93, 485–498.

Westra, S., L. Alexander, and F. Zwiers, 2013: Global increasing trends in annual maximum daily precipitation. *Journal of Climate*, **26**, 3904–3918.

Yoshioka, N., K. Ide, M. Morita, and Y. Hirabayashi, 2020: Climate change impacts on heavy precipitation and urban flooding. *Journal of Japan society of civil engineers Series B1*, 76, 55–60 (in Japanese).

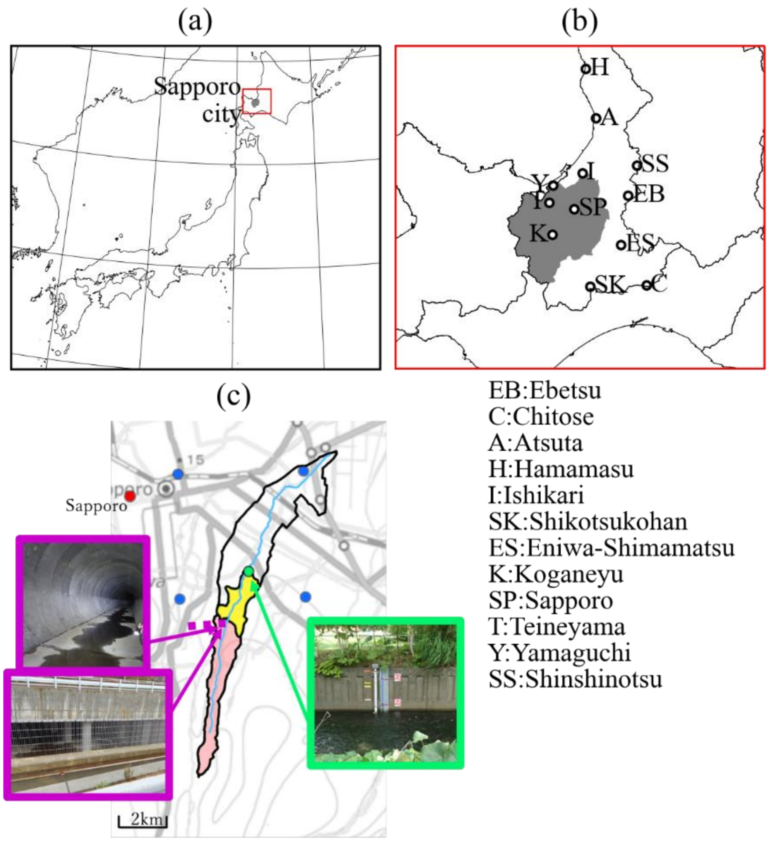

Figure 1: (a) Map and (b) zoom-in map and (c) pictures around the Motsukisamu River. Sapporo City was shaded in (a) and (b). Circles in (b) denote the location of Automated Meteorological Data Acquisition System (AMeDAS) observation points in Ishikari area described below. Black line in (c) is the Motsukisamu River basin and purple dotted line is the aqueduct tunnel in the upstream. The river model is constructed for the pink and yellow areas, and the rainfall in the yellow area partly flows out by the tunnel. Green, red, and blue dots show the observation point of precipitation and water level, AMeDAS observation point of Sapporo, and the neighbor grid-points of d4PDF surrounding the site, respectively.

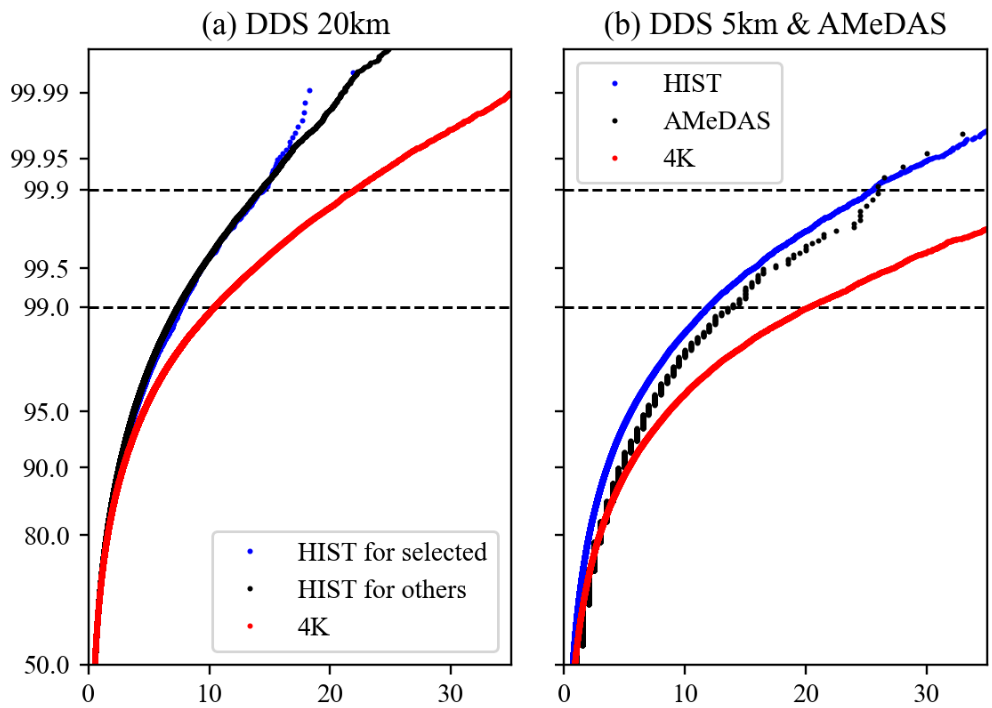

Figure 2: (a) The quantile-quantile (Q-Q) plot of hourly precipitation in June-July-August-September months at Sapporo in 20-km d4PDF historical simulation (blue) for years selected in the 5-km downscaling and (black) for other years and (red) in 20-km d4PDF 4K simulation. (b) The Q-Q plot of hourly precipitation at Sapporo (blue) historical and (red) 4K experiments in 5-km downscaling and (black) AMeDAS observation from 1991 to 2020. All the statistics were taken for hours where the precipitation exceeded 0.1 mm.

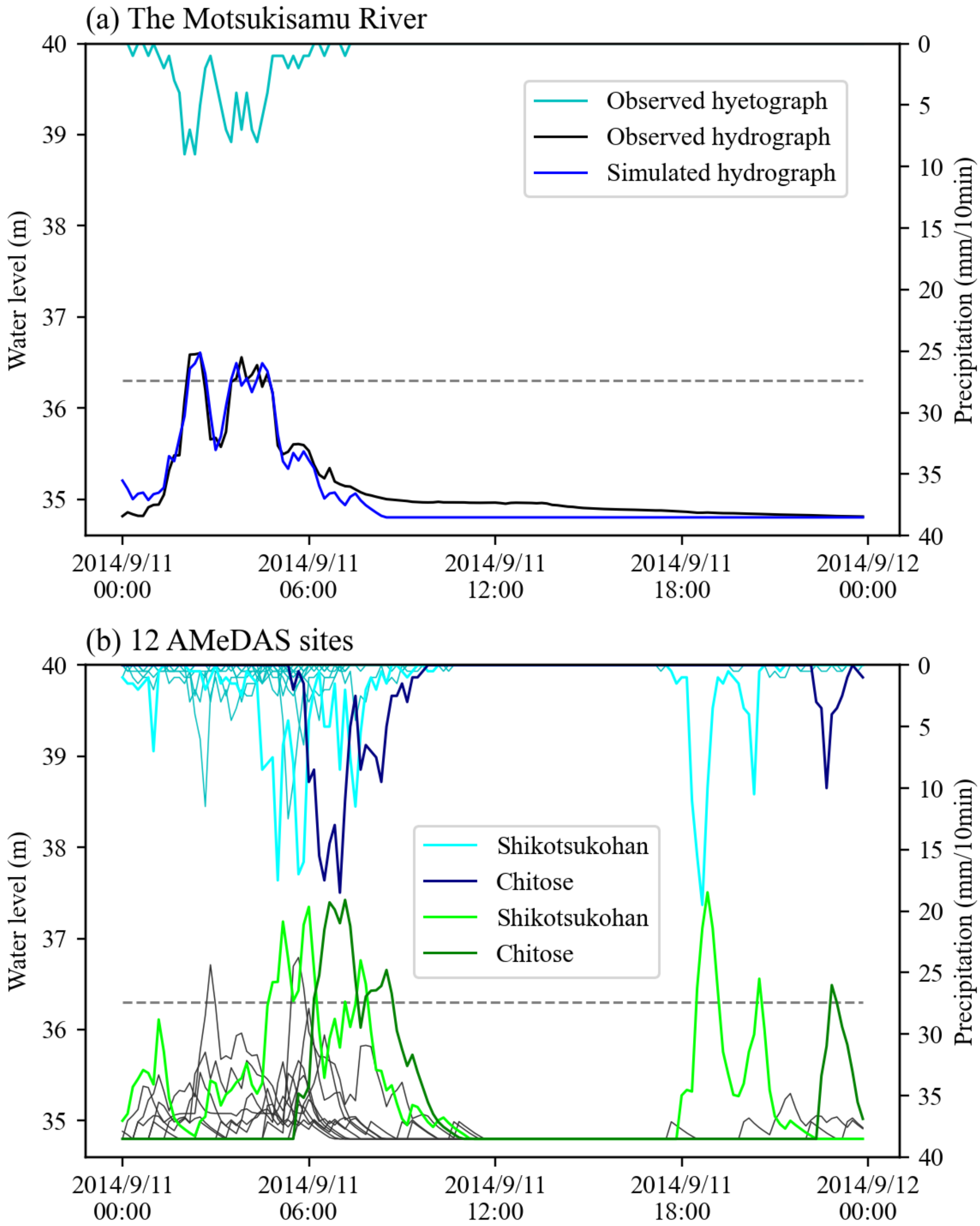

Figure 3: Hyetograph and hydrograph on September 11, 2014, at the Motsukisamu River under historical climate. (a) (Line in the upper side) Rainfall and (black line) water level observed at the Motsukisamu River. Blue line shows the water level in the reference simulation. Gray dotted line shows the flood stage level 4. (b) Same as (a), but the results for “ensemble” simulation with precipitation observed in 12 sites of Ishikari area. Shikotsukohan and Chitose sites were emphasized by coloring as legend.

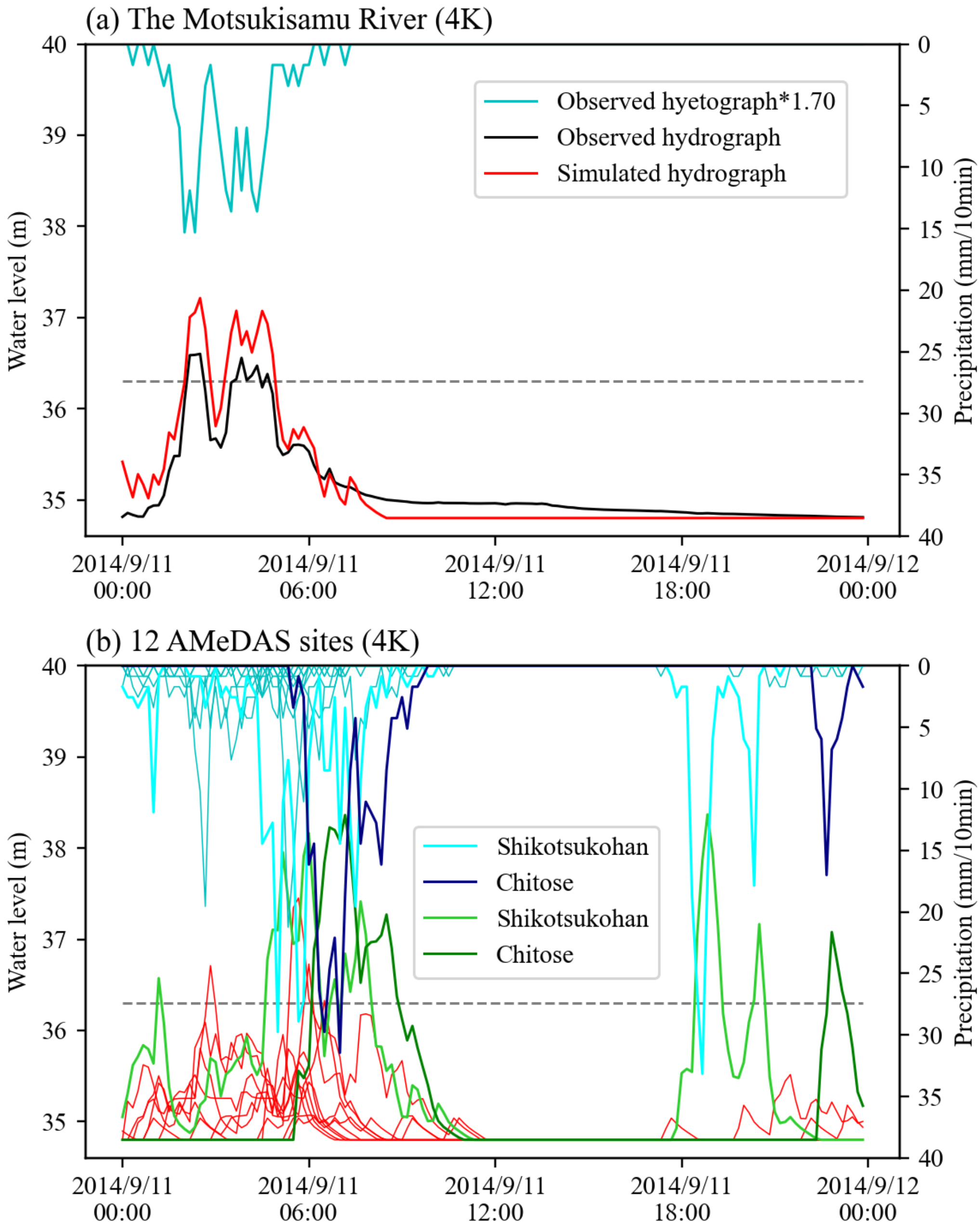

Figure 4: Same as Fig. 3, but for +4 K climate.

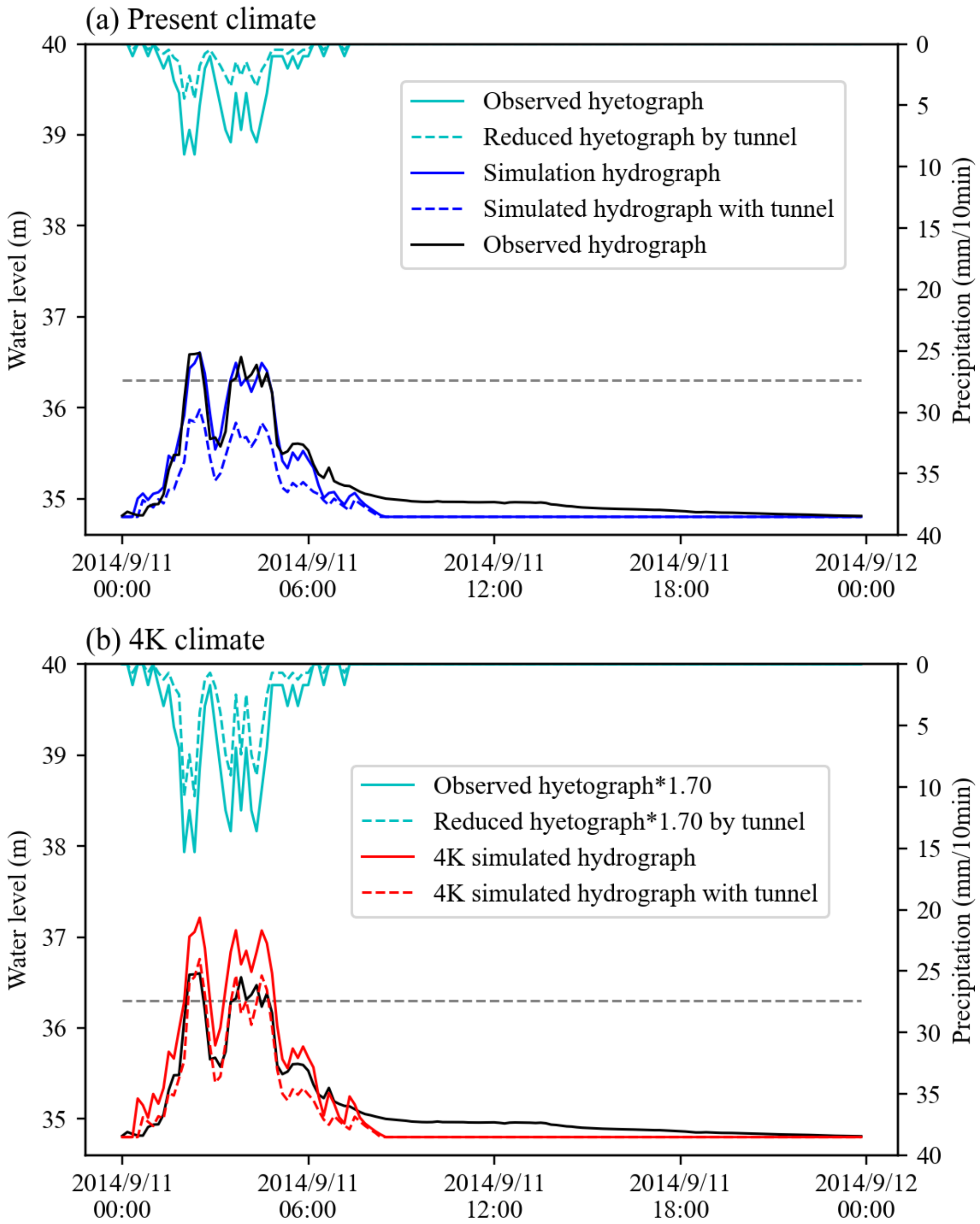

Figure 5: (a; dotted lines) The net precipitation inversely estimated considering the amount of the removal of water through the aqueduct tunnel and the simulated water level forced by the net precipitation. The hyetograph and hydrograph in the reference experiment were superimposed with solid lines. (b) Same as (a), but all under +4 K

climate. Note that the hydrograph is colored red in (b). The black line is the observed water level as a reference.